Ni(II), Cu(II), and Zn(II) Dinuclear Metal Complexes with an Aza−Phenolic Ligand: Crystal Structures, Magnetic Properties, and Solution Studies

ARTICLE *in* INORGANIC CHEMISTRY · FEBRUARY 2003

Impact Factor: 4.76 · DOI: 10.1021/ic0204070 · Source: PubMed

12 AUTHORS, INCLUDING:

Andrea Caneschi
University of Florence
417 PUBLICATIONS **18,333** CITATIONS
SEE PROFILE

Mauro Formica
Università degli Studi di Urbino "Carlo Bo"
61 PUBLICATIONS **1,046** CITATIONS
SEE PROFILE

Vieri Fusi
Università degli Studi di Urbino "Carlo Bo"
143 PUBLICATIONS **2,708** CITATIONS
SEE PROFILE

Annalisa Guerri Dr
University of Florence
68 PUBLICATIONS **954** CITATIONS
SEE PROFILE

Inorg. Chem. **2003**, *42*, 348–357

Ni(II), Cu(II), and Zn(II) Dinuclear Metal Complexes with an Aza–Phenolic Ligand: Crystal Structures, Magnetic Properties, and Solution Studies

Elisabetta Berti,[†] Andrea Caneschi,[†] Carole Daiguebonne,[‡] Paolo Dapporto,[§] Mauro Formica,[||] Vieri Fusi,*[,||] Luca Giorgi,[||] Annalisa Guerri,[§] Mauro Micheloni,*[,||] Paola Paoli,[§] Roberto Pontellini,[||] and Patrizia Rossi[§]

Department of Chemistry, University of Florence, Via della Lastruccia 5, I-50019 Sesto Fiorentino (Fi), Italy, GRCM "Chimie Inorganique des Lanthanides", INSA, CS 14315, 35043 Rennes Cedex, France, Department of Energy Engineering "Sergio Stecco", University of Florence, Via S. Marta 3, I-50139 Florence, Italy, and Institute of Chemical Sciences, University of Urbino, P.za Rinascimento 6, I-61029 Urbino, Italy

Received June 17, 2002

The basicity behavior and ligational properties of the ligand 2-((bis(aminoethyl)amino)methyl)phenol (**L**) toward Ni(II), Cu(II), and Zn(II) ions were studied by means of potentiometric measurements in aqueous solution (298.1 ± 0.1 K, $I = 0.15$ mol dm^{-3}). The anionic $\mathbf{L}_{-H}^{-}$ species can be obtained in strong alkaline solution; this species behaves as tetraprotic base (log $K_1 = 11.06$, log $K_2 = 9.85$, log $K_3 = 8.46$, log $K_4 = 2.38$). **L** forms mono- and dinuclear complexes in aqueous solution with all the transition metal ions examined; the dinuclear species show a $[M_2(\mathbf{L}_{-H})_2]^{2+}$ stoichiometry in which the ligand/metal ratio is 2:2. The studies revealed that two mononuclear $[M\mathbf{L}_{-H}]^{+}$ species self-assemble, giving the dinuclear complexes, which can be easily isolated from the aqueous solution due to their low solubility. This behavior is ascribed to the fact that **L** does not fulfill the coordination requirement of the ion in the mononuclear species and to the capacity of the phenolic oxygen, as phenolate, to bridge two metal ions. All three dinuclear species were characterized by determining their crystal structures, which showed similar coordination patterns, where all the single metal ions are substantially coordinated by three amine functions and two oxygen atoms of the phenolate moieties. The two metals in the dinuclear complexes are at short distance interacting together as shown by magnetic measurements performed with Ni(II) and Cu(II) complexes, which revealed an antiferromagnetic coupling between the two metal ions. The $[Cu_2(\mathbf{L}_{-H})_2]^{2+}$ cation shows a phase transition occurring by the temperature between 100 and 90 K; the characterization of the compounds existing at different temperatures was investigated using X-ray single-crystal diffraction, EPR, and magnetic measurements.

Introduction

Dinuclear metal complexes and ligands capable of giving them have been extensively investigated due to their potential practical applications in many fields of chemistry.[1−5] They are used as model systems for active centers of many metalloenzymes[6−8] and as successful devices to host and carry small molecules or ions and as catalysts.[9−12] Moreover, they show independent chemistry compared with the mononuclear complex giving often rise to peculiar optical and

* To whom correspondence should be addressed. E-mail: vieri@chim.uniurb.it (V.F.).
[†] Department of Chemistry, University of Florence.
[‡] GRCM "Chimie Inorganique des Lanthanides", INSA.
[§] Department of Energy Engineering "Sergio Stecco", University of Florence.
[||] Institute of Chemical Sciences, University of Urbino.

(1) (a) Pedersen, C. J. *J. Am. Chem. Soc.* **1967**, *89*, 7017. (b) Lehn, J. M. *Pure Appl. Chem.* **1977**, *49*, 857. (c) Cram D. J.; Cram, J. M. *Science* **1984**, *183*, 4127. (d) Lehn, J. M. *Angew. Chem., Int. Ed. Engl.* **1988**, *27*, 89.
(2) (a) Bianchi, A.; Bowman-James, K.; Garcia-España, E. *Supramolecular Chemistry of Anions*; Wiley-VCH: New York, 1997. (b) Lehn, J. M. *Supramolecular Chemistry, Concepts and Perspectives*; VCH: Weinheim, Germany, 1995.
(3) (a) Guerriero, P.; Tamburini, S.; Vigato, P. A. *Coord. Chem. Rev.* **1995**, *110*, 17. (b) Bazzicalupi, C.; Bencini, A.; Fusi, V.; Giorgi, C.; Paoletti, P.; Valtancoli, B. *Inorg. Chem.* **1998**, *37*, 941 and references therein.
(4) (a) He, H.; Martell, A. E.; Motekaitis, R. J.; Reibespiens, J. J. *Inorg. Chem.* **2000**, *39*, 1586. (b) Koike, T.; Inoue, M.; Kimura, E.; Shiro, M. *J. Am. Chem. Soc.* **1996**, *118*, 3091.

10.1021/ic0204070 CCC: $25.00
Published on Web 12/21/2002

magnetic properties. Parameters that can be acted on to achieve desired chemical behaviors include the nature of the metal ions, the distance between them, and their coordination requirement. However, it should be taken into account that one of the requirements to assemble external species is an unsaturated coordination environment of the single coordinated metal ion.

Many of the ligands able to bind two metal ions and permit them to interact and/or cooperate in their molecular framework are macrocycles. Owing to the intriguing structural topologies of molecules leading to the formation of dinuclear complexes, we recently synthesized ligands having or not having macrocyclic characteristics enabling them to form dinuclear complexes. By exploitation of the capability of the phenol oxygen to bridge metal ions, these ligands are able to bind two transition metal ions in close proximity (Chart 1) and were used for various applications.[13] In particular we observed that, in aqueous solution with Cu(II) ion, **L2** forms stable dinuclear complexes having a ligand/metal ratio of 2:2 in which the two copper ions are located very close to each other.[14] Following the idea of producing dinuclear metal complexes using a ligand/metal ratio of 2:2 in which two mononuclear M**L** species can self-assemble to form $(M\mathbf{L})_2$ dinuclear species, we chose the simple asymmetric ligand 2-((bis(aminoethyl)amino)methyl)phenol (**L**) containing the phenol moiety coupled with a triaminic fragment. **L** can be seen as the noncyclic counterpart of **L2**, and in this work its binding properties toward the bipositive ions Ni(II), Cu(II), and Zn(II) were studied.

Chart 1

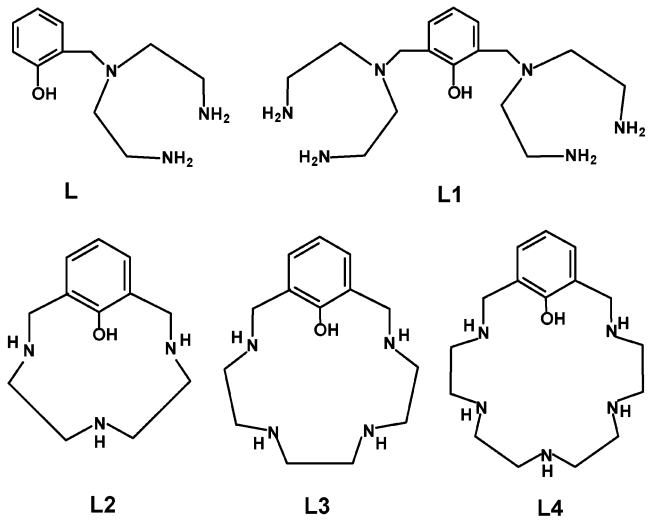

This molecule shows a surprising ability to assemble two transition metal ions in close proximity following an overall reaction of 2 ligand molecules + 2 metal ions. The dinuclear species are formed in aqueous solution and can be easily obtained as crystalline solids. Solid-state characterization of the isolated compounds was performed using single-crystal X-ray diffraction, EPR, and magnetic measurement techniques.

Experimental Section

General Methods. UV absorption spectra were recorded at 298 K on a Varian Cary-100 spectrophotometer equipped with a temperature control unit. ESI mass spectra were recorded on a ThermoQuest LCQ Duo LC/MS/MS spectrometer. IR spectra were recorded on a Shimadzu FTIR-8300 spectrometer in the range 400−4000 cm^{-1} having resolution of 1.0 cm^{-1}. ^1H and ^{13}C NMR spectra were recorded on a Bruker AC-200 instrument, operating at 200.13 and 50.33 MHz, respectively. For the ^1H and ^{13}C NMR experiment in CD_3OD, the peak positions are reported with respect to TMS. All reagents and solvents used were of analytical grade.

X-ray Crystallography. Crystallographic data for **1**−**3** were collected on a Siemens P4 diffractometer using graphite-monochromated Cu Kα radiation ($\lambda = 1.5418$ Å), $T = 298$ K. Intensity data were corrected for Lorentz and polarization effects. Structures were solved by direct methods using the SIR97 program[15] and refined by full-matrix least squares against F^2 using all data (SHELX97[16]). In all cases, anisotropic thermal parameters were used for the non-H atoms while an overall isotropic thermal parameter was used for the hydrogen ones. These latter were introduced in calculated positions, and their temperature factors were fixed accordingly to the corresponding values of their bonded atoms. Absorption corrections were performed with the program DIFABS.[17]

In addition, crystallographic data for sample **2** were collected at 80 K (hereafter this compound will be referred to as **2′**) on a Nonius Kappa CCD diffractometer using a Mo Kα radiation ($\lambda = 0.710\ 73$ Å). Its structure was solved by a direct method using SHELXS97

(5) (a) Bazzicalupi, C.; Bencini, A.; Bianchi, A.; Fusi, V.; Garcia-España, E.; Giorgi, C.; Llinares, J. M.; Ramirez, J. A.; Valtancoli,B. *Inorg. Chem.* **1999**, *38*, 620 and references therein. (b) Meyer, F.; Winter, R. F.; Kaifer, E. *Inorg. Chem.* **2001**, *40*, 4597.
(6) (a) Lippard, S. J.; Berg, J. M. *Principles of Bioinorganic Chemistry*; University Science Books: Mill Valley, CA, 1994. (b) *Bioinorganic Catalysis*; Reedijk, J., Ed.; Dekker: New York, 1993.
(7) (a) Karlin, K. D. *Science* **1993**, *261*, 701. (b) Wilcox, D. E. *Chem. Rev.* **1996**, *96*, 2435. (C) Hughes, M. N. *The Inorganic Chemistry of the Biological Processes*; Wiley: New York, 1981.
(8) (a) Agnus, Y. L. *Copper Coordination Chemistry: Biochemical and Inorganic Perspective*; Adenine Press: Guilderland, NY, 1983. (b) Bertini, I., Luchinat, C., Marek, W., Zeppezauer, M., Eds. *Zinc Enzymes*; Birkauser: Boston, MA, 1986.
(9) (a) Martell, A. E.; Sawyer, D. T. *Oxygen Complexes and Oxygen Activation by Transition Metals*; Plenum Press: New York, 1987. (b) Schindler, S. *Eur. J. Inorg. Chem.* **2000**, 2311. (c) Davies, M. B. *Coord. Chem. Rev.* **1996**, 1. (c) Aoki, S.; Kimura, E. *J. Am. Chem. Soc.* **2000**, *122*, 4542.
(10) (a) Meyer, F.; Rutsch, P. *Chem. Commun*. **1998**, 1037 (b) Karplus, P. A.; Pearson, M. A.; Hausinger, R. P. *Acc. Res. Chem.* **1997**, *30*, 330. (c) Musiani, M.; Arnolfi, E.; Casadio, R.; Ciurli, S. *J. Biol. Inorg. Chem.* **2001**, *6*, 300.
(11) (a) Cooksey, C. J.; Garratt, P. J.; Land, E. J.; Pavel, S.; Ramsden, C. A.; Riley, P. A.; Smit, N P. M. *J. Biol. Chem*. **1997**, *272*, 26226. (b) Sayre, L. M.; Nadkarni, D. V. *J. Am. Chem. Soc*. **1994**, *116*, 3157. (c) Sánchez-Ferrer, A.; Rodríguez-López, J. N.; García-Cánovas, F.; García-Carmona, F. *Biochim. Biophys. Acta* **1995**, *1247*, 1.
(12) (a) Barrios, A. M.; Lippard, S. J. *J. Am. Chem. Soc*. **2000**, *122*, 9172. (b) Barrios, A. M.; Lippard, S. J. *Inorg. Chem.* **2001**, *40*, 1250.
(13) (a) P. Dapporto, M. Formica, V. Fusi, M. Micheloni, P. Paoli, R. Pontellini, P. Romani, P. Rossi, *Inorg. Chem.* **2000**, *39*, 2156. (b) Ceccanti, N.; Formica, M.; Fusi, V.; Micheloni, M.; Pardini, R.; Pontellini, R.; Tinè, M. R. *Inorg. Chim. Acta* **2001**, *321*, 153. (c) Dapporto, P.; Formica, M.; Fusi, V.; Micheloni, M.; Paoli, P.; Pontellini, R.; Rossi, P. *Inorg. Chem.* **2000**, *39*, 4663. (d). Formica, V. Fusi, L. Giorgi, M. Micheloni, P. Palma, R. Pontellini, *Eur. J. Org. Chem.* **2002**, 402.
(14) Fusi, V.; Llobet, A.; Mahia, J.; Micheloni, M.; Paoli, P.; Ribas, X.; Rossi, P. *Eur. J. Inorg. Chem.* **2002**, *4*, 987.
(15) Altomare A.; Cascarano, G. L.; Giacovazzo, C.; Guagliardi, A.; Burla, M. C.; Polidori, G.; Camalli, M. *J. Appl. Crystallogr.* **1999**, *32*, 115.
(16) Sheldrick, G. M. *SHELX 97*; University of Göttingen: Göttingen, Germany, 1997.
(17) Walker, N.; Stuart, D. D. *Acta Crystallogr., Sect. A* **1993**, *39*, 158.

Table 1. Crystal Data and Structure Refinement for **1**, **2**, **2′**, and **3**

param	identification code			
	1	**2**	**2′**	**3**
empirical formula	$C_{22}H_{38}Cl_2N_6Ni_2O_{11}$	$C_{22}H_{36}Cl_2Cu_2N_6O_{10}$	$C_{22}H_{36}Cl_2Cu_2N_6O_{10}$	$C_{22}H_{36}Cl_2Zn_2N_6O_{10}$
fw	750.90	742.54	742.54	746.21
temp (K)	298	298	80	298
wavelength (Å)	1.54184	1.54184	0.71073	1.54184
cryst system	orthorhombic	monoclinic	triclinic	monoclinic
space group	$Pc2_1b$	$P2_1/n$	$P\bar{1}$	$P2_1$
a (Å)	15.242(2)	8.991(6)	8.99(2)	9.467(1)
b (Å)	10.593(2)	9.889(2)	9.615(8)	13.846(1)
c (Å)	19.072(4)	16.643(4)	16.65(4)	11.616(1)
α (deg)	90	90	88.1(2)	90
β (deg)	90	94.04(4)	84.9(2)	95.205(7)
γ (deg)	90	90	88.96(1)	90
V (Å^3), Z	3079(1), 4	1476(1), 2	1432.81(1), 2	1516.3(2), 2
D_c (Mg/m^3)	1.620	1.671	1.721	1.634
μ (mm^{-1})	3.687	3.997	1.736	4.107
F(000)	1560	764	764	768
cryst size (mm)	0.4 × 0.4 × 0.5	0.4 × 0.5 × 0.7	0.3 × 0.4 × 0.4	0.5 × 0.6 × 0.6
θ range (deg)	4.17−64.17	5.21−64.24	3.09−28.47	3.82−64.36
reflcns collcd/unique	2891/2679	3241/2346	29 129/6640	3293/2775
data/restraints/params	2690/1/399	2161/0/219	16 104/0/381	2351/1/381
final R indices [$I > 2\sigma(I)$]	R1 = 0.0400	R1 = 0.0508	R1 = 0.1214	R1 = 0.0643
	wR2 = 0.1083	wR2 = 0.1303	wR2 = 0.3121	wR2 = 0.1638
R indices (all data)	R1 = 0.0437	R1 = 0.0537	R1 = 0.2085	R1 = 0.0781
	wR2 = 0.1123	wR2 = 0.1351	wR2 = 0.3838	wR2 = 0.1818

and then refined by full-matrix least squares against F^2 using all data (SHELX97). Anisotropic thermal parameters were used for all non-hydrogen atoms, while the hydrogen atoms were introduced in calculated positions. Their positions, as well as their isotropic temperature factors, were refined in accordance with the linked atoms.

In all cases geometrical calculations were performed by PARST97[18] and molecular plots were produced by the ORTEP3 program.[19] Table 1 reports details of the crystal data, data collection, structure solution, and refinement.

For compound **1** it was found that the carbon atom labeled as C(22) has two different positions, indicating a region of disorder in the molecule: a population parameter of 0.5 was assigned to each one.

Three oxygen atoms of the perchlorate anion in compound **2** were found to be disordered in the refined model, and two different positions for each atom were assigned with a population factor of 0.5.

The solid-state structure of compound **2′** showed a phase transformation from the monoclinic system to the triclinic. Cell parameters were determined every 10 K from room temperature to 80 K, and the phase transition was found to occur between 100 and 90 K. Moreover, the crystal showed a twinning due to a twin axis along b (rotation twin). The data file was created by the EvalCCD program from the CCD package.[20]

The correct enantiomer of compound **3** was identified by the value of the Flack parameter.

EMF Measurements. Equilibrium constants for protonation and complexation reactions with **L** were determined by pH-metric measurements (pH = −log [H$^+$]) in 0.15 mol dm^{-3} NaCl at 298.1 ± 0.1 K, using the fully automatic equipment that has already been described;[21] the EMF data were acquired with the PASAT computer program.[22] The combined glass electrode was calibrated as a hydrogen concentration probe by titrating known amounts of HCl with CO_2-free NaOH solutions and determining the equivalent point by Gran's method,[23] which gives the standard potential $E°$ and the ionic product of water (pK_w = 13.73(1) at 298.1 K in 0.15 mol dm^{-3} NaCl, K_w = [H$^+$][OH$^-$]). At least three potentiometric titrations were performed for each system in the pH range 2−11, and all titrations were treated either as single sets or as separate entities, for each system; no significant variations were found in the values of the determined constants. The HYPERQUAD computer program was used to process the potentiometric data.[24]

Magnetic Measurements. The temperature dependence of the magnetic susceptibility was measured on a Cryogenics S600 SQUID magnetometer in the temperature range of 300−2.5 K. Diamagnetic corrections of the constituent atoms were estimated from Pascal constants[25] respectively as −307 × 10^{-6} (**1**) and −295 × 10^{-6} (**2**) emu mol^{-1} G^{-1}.

EPR Spectra. X-band (9 GHz) EPR spectra were recorded with a Varian E9 spectrometer equipped with an Oxford instrument liquid-helium continuous-flow cryostat in the temperature range 300−4.2 K.

Synthesis of Complexes. 2-((bis(2-aminoethyl)amino)methyl)-phenol (**L**) was prepared as previously described.[26]

[Ni$_2$(L$_{-H}$)$_2$](ClO$_4$)$_2$(H$_2$O) (1). A sample of Ni(ClO$_4$)$_2$·6H$_2$O (182 mg, 0.5 mmol) in water (20 mL) was added to an aqueous solution (30 mL) of **L**·3HCl (159 mg, 0.5 mmol). The pH of the resulting solution was adjusted to 8 with 0.1 M NaOH, and then NaClO$_4$·H$_2$O (29 mg, 0.2 mmol) was added. After a few minutes, **1** precipitated as a microcrystalline greenish-blue solid (171 mg, 91%). Crystals suitable for X-ray analysis were obtained by slow evaporation of the solvent of an aqueous diluted solution of **1**. Anal. Calcd for $C_{22}H_{38}Cl_2N_6Ni_2O_{11}$: C, 35.19; H, 5.10; N, 11.19.

(18) Nardelli, M. *Comput. Chem.* **1983**, *7*, 95.
(19) Farrugia, L. J. *J. Appl. Crystallogr.* **1997**, *30*, 565.
(20) *Nonius, COLLECT: Kappa CCD software*; Nonius BV: Delft, The Netherlands, 1998.
(21) Dapporto, P.; Fusi, V.; Micheloni, M.; Palma, P.; Paoli, P.; Pontellini, R. *Inorg. Chim. Acta* **1998**, *275*−*276*, 168.
(22) Fontanelli, M.; Micheloni, M. *1st Spanish-Italian Congress: Thermodynamics of Metal Complexes*, Peñiscola, Spain, June 3−6, 1990; University of Valencia: Valencia, Spain, 1990; p 41.
(23) (a) Gran, G. *Analyst* **1952**, *77*, 661. (b) Rossotti, F. J.; Rossotti, H. *J. Chem. Educ.* **1965**, *42*, 375.
(24) Gans, P.; Sabatini, A.; Vacca, A. *Talanta* **1996**, *43*, 1739.
(25) O′Connor, C. J. *Prog. Inorg. Chem.* **1982**, *29*, 203
(26) Zeng, K.; Qian, M.; Gou, S.; Fun, H.-K.; Duan, C.; You, X. *Inorg. Chim. Acta* **1999**, *294*, 1.

Found: C, 35.24; H, 5.06; N, 11.23. FT-IR: 3339 s and 3291 s (N−H, ν), 2923 w (C−H, ν), 1594 s (H−N−H, δ), 1572 w, 1481 s and 1472 s (C═C, ν), 1276 s, 1242 w (C−O, C−N, ν), 1090 s (Cl−O, ν), 872 m, 783 m, and 750 m (C−H, π), and 770 m (Ni−O−Ni, ν) cm^{-1}. MS (ESI) (*m*/*z*): 632−634 (($Ni\mathbf{L}_{-H})_2ClO_4^+$), 267 (($Ni\mathbf{L}_{-H})_2^{2+}$).

$[Cu_2(\mathbf{L}_{-H})_2](ClO_4)_2$ (2). This compound was synthesized from **L**·3HCl (159 mg, 0.5 mmol) and $Cu(ClO_4)_2 \cdot 6H_2O$ (185 mg, 0.5 mmol) by following the same procedure reported for **1**, giving **2** as green microcrystals (160 mg, 89%). Crystals suitable for X-ray analysis were obtained by slow evaporation of the solvent of an aqueous diluted solution of **2**. Anal. Calcd for $C_{22}H_{36}Cl_2Cu_2N_6O_{10}$: C, 35.59; H, 4.89; N, 11.32. Found: C, 35.64; H, 4.85; N, 11.43. FT-IR: 3342 s and 3292 s (N−H, ν), 2925 w (C−H, ν), 1594 s (H−N−H, δ), 1569 w, 1480 s and 1451 s (C═C, ν), 1276 s, 1243 w (C−O, C−N, ν), 1089 s (Cl−O, ν), 892 m, 789 m, and 750 m (C−H, π), and 769 m (Cu−O−Cu, ν) cm^{-1}. MS (ESI) (*m*/*z*): 642−644 (($Cu\mathbf{L}_{-H})_2ClO_4^+$), 271.8 (($Cu\mathbf{L}_{-H})_2^{2+}$).

$[Zn_2(\mathbf{L}_{-H})_2(ClO_4)_2]$ (3). This compound was synthesized from **L**·3HCl (159 mg, 0.5 mmol) and $Zn(ClO_4)_2 \cdot 6H_2O$ (186 mg, 0.5 mmol) by following the same procedure reported for **1** giving **3** as colorless microcrystals (157 mg, 84%). Crystals suitable for X-ray analysis were obtained by slow evaporation of the solvent of an aqueous diluted solution of **3**. Anal. Calcd for $C_{22}H_{36}Cl_2Zn_2N_6O_{10}$: C, 35.41; H, 4.86; N, 11.26. Found: C, 35.36; H, 4.93; N, 11.32. ^{1}H NMR (CD_3OD, 25 °C): 2.70 (t, 8H), 2.89 (t, 8H), 3.80 (s, 4H), 6.60 (t, 2H), 6.75 (d, 2H), 7.02 (d, 2H), 7.11 (t, 2H), ppm. ^{13}C NMR (ppm): 38.6, 53.5, and 58.3 (aliphatic resonances), 117.8, 121.4, 127.0, 131.2, 132.7, 165.3 (aromatic resonances). FT-IR: 3342 s and 3285 s (N−H, ν), 2923 w (C−H, ν), 1595 s (H−N−H, δ), 1574 w, 1481 s and 1449 s (C═C, ν), 1266 s, 1241 w (C−O, C−N, ν), 1091 s (Cl−O, ν), 876 m, 781 m and 752 m (C−H, π), and 765 m (Zn−O−Zn, ν) cm^{-1}. MS (ESI) (*m*/*z*): 646−648 (($Zn\mathbf{L}_{-H})_2ClO_4^+$), 273.5 (($Zn\mathbf{L}_{-H})_2^{2+}$).

Caution! *Perchlorate salts of organic compounds are potentially explosive; these compounds must be prepared and handled with great care!*

Results and Discussion

Synthesis. The three dinuclear complexes of formula $[M_2(\mathbf{L}_{-H})_2](ClO_4)_2 \cdot nH_2O$ ($n = 1$ for Ni(II), $n = 0$ for Cu(II) and Zn(II), respectively) were obtained almost quantitatively with the same strategy, by precipitating them from their aqueous solution in the pH range where such species are present in solution. Although they coexist in aqueous solution with the mononuclear species (see Figure 7), the dinuclear complexes can be isolated in high yield in the solid state, probably due to their lower solubility in aqueous solution with respect to the mononuclear species.

Description of the Structures. $[Ni_2(\mathbf{L}_{-H})_2](ClO_4)_2(H_2O)$ (1). The asymmetric unit contains the dinuclear complex, which is a dimer with stoichiometry $[Ni_2(\mathbf{L}_{-H})_2]^{2+}$, two perchlorate anions, and a water molecule. Each nickel ion is coordinated by the nitrogen atoms from the amino arm of the ligand and by the two oxygen atoms provided by the phenol rings, cis-equatorially coordinated and acting as bridging unit between the two metal ions (Figure 1), which are 3.044(1) Å apart. The Ni···O and Ni···N distances (Table 2) are in agreement with those found for analogous Ni(II) complexes having the same set of donor atoms retrieved by a search in the Cambridge Structural Database (CSD), V. 5.21.[27] The mean planes described by the atoms of the two phenolate moieties are at 106.8(3)° with respect to each other. The coordination geometry of both nickel ions could be described as an irregular square pyramid (sp), as revealed by the trigonal index,[28] τ, of 0.15 and 0.09 for Ni(1) and Ni(2), respectively (for perfect square pyramidal and bipyramidal geometries, the τ values are zero and unity,

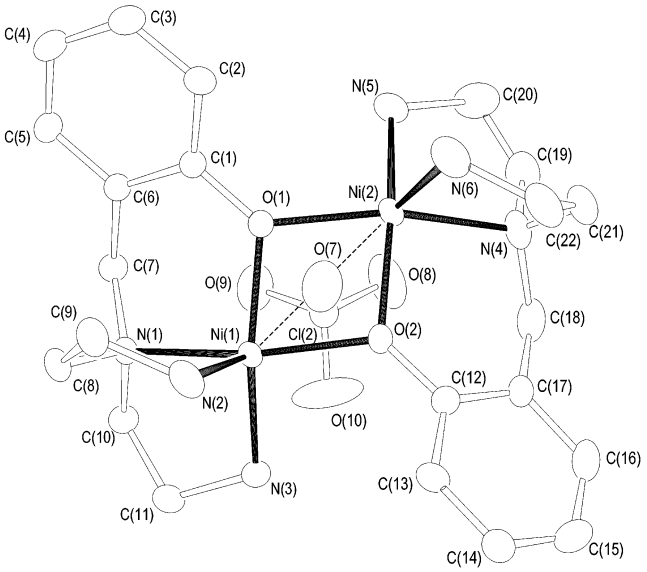

Figure 1. ORTEP-3 view of the complex cation $[Ni_2(\mathbf{L}_{-H})_2]^{2+}$. Thermal ellipsoids are at 30% probability.

Table 2. Selected Bond Lengths (Å) and Angles (deg) for **1** and **3**

1		**3**	
Ni(1)−Ni(2)	3.044(1)	Zn(1)−Zn(2)	3.140(2)
Ni(1)−O(1)	1.988(4)	Zn(1)−O(1)	1.999(9)
Ni(1)−O(2)	2.001(4)	Zn(1)−O(2)	2.034(8)
Ni(1)−N(1)	2.080(4)	Zn(1)−N(1)	2.18(1)
Ni(1)−N(2)	2.026(6)	Zn(1)−N(2)	2.07(1)
Ni(1)−N(3)	2.062(5)	Zn(1)−N(3)	2.05(1)
Ni(2)−O(1)	1.993(4)	Zn(2)−O(1)	2.048(7)
Ni(2)−O(2)	1.977(4)	Zn(2)−O(2)	2.01(1)
Ni(2)−N(4)	2.087(5)	Zn(2)−N(4)	2.176(9)
Ni(2)−N(5)	2.042(5)	Zn(2)−N(5)	2.06(1)
Ni(2)−N(6)	2.047(7)	Zn(2)−N(6)	2.06(1)
O(1)−Ni(1)−O(2)	78.0(2)	O(1)−Zn(1)−O(2)	78.4(3)
O(1)−Ni(1)−N(1)	94.1(2)	O(1)−Zn(1)−N(1)	89.9(4)
O(1)−Ni(1)−N(2)	98.4(2)	O(1)−Zn(1)−N(2)	110.5(4)
O(1)−Ni(1)−N(3)	157.2(2)	O(1)−Zn(1)−N(3)	131.9(5)
O(2)−Ni(1)−N(1)	166.5(2)	O(2)−Zn(1)−N(1)	165.1(4)
O(2)−Ni(1)−N(2)	106.8(2)	O(2)−Zn(1)−N(2)	110.0(4)
O(2)−Ni(1)−N(3)	98.6(2)	O(2)−Zn(1)−N(3)	97.7(4)
N(2)−Ni(1)−N(1)	84.9(2)	N(2)−Zn(1)−N(1)	82.5(4)
N(2)−Ni(1)−N(3)	104.1(3)	N(3)−Zn(1)−N(2)	115.7(5)
N(3)−Ni(1)−N(1)	84.5(2)	N(3)−Zn(1)−N(1)	83.3(4)
O(2)−Ni(2)−O(1)	78.5(2)	O(2)−Zn(2)−O(1)	77.9(3)
O(1)−Ni(2)−N(4)	163.0(2)	O(1)−Zn(2)−N(4)	163.4(4)
O(1)−Ni(2)−N(5)	98.5(2)	N(5)−Zn(2)−O(1)	97.2(4)
O(1)−Ni(2)−N(6)	110.1(2)	O(1)−Zn(2)−N(6)	111.9(4)
O(2)−Ni(2)−N(4)	91.7(2)	O(2)−Zn(2)−N(4)	90.0(4)
O(2)−Ni(2)−N(5)	157.5(2)	O(2)−Zn(2)−N(5)	130.7(4)
O(2)−Ni(2)−N(6)	101.4(2)	O(2)−Zn(2)−N(6)	112.8(5)
N(5)−Ni(2)−N(4)	85.3(2)	N(5)−Zn(2)−N(4)	82.1(4)
N(5)−Ni(2)−N(6)	100.5(3)	N(5)−Zn(2)−N(6)	114.3(5)
N(6)−Ni(2)−N(4)	85.3(3)	N(6)−Zn(2)−N(4)	83.1(4)

(27) Allen, F. H.; Kennard, O. Cambridge Structural Database. *J. Chem. Soc., Perkin Trans. 2* **1989**, 1131.
(28) Addison, A. W.; Rao, T. N.; Reedijk, J.; Van Rijn, J.; Vershcoor, G. C. *J. Chem. Soc., Dalton Trans.* **1984**, 1349.

respectively). The sets of four atoms N(1), N(3), O(1), O(2) and N(4), N(5), O(1), O(2) describe each base [the maximum deviations from the mean planes are −0.132(6) Å for N(3) and 0.092(7) Å for N(4)], with both the apical donors, N(2) and N(6), lying in the same spatial region with respect to the Ni_2O_2 grouping. In this respect it is noteworthy that the region below each axial donor is occupied by a perchlorate counterion, whose oxygen atom O(7) points quite straight toward the Ni_2O_2 moiety. Given that the oxygen−nickel bond distances are less than the sum of their van der Waals radii, even if significantly longer than the usual Ni−O bond lengths (2.906(7) and 2.831(7) Å, for O(7)−Ni(1) and O(7)−Ni(2), respectively), each Ni(II) ion could be described as 5 + 1 coordinated (Figure 1). In fact the perchlorate oxygen atom takes up both the sixth positions of two quite irregular octahedrons around each metal ion (∠N(2)−Ni(1)−O(7) 167.5(2)°, <N(6)−Ni(2)−O(7) 177.2(2)°).

As regards crystal packing, each complexed cation is surrounded by four different perchlorate anions, whose oxygen atoms are interacting with the hydrogen atoms of the primary nitrogen atoms of the ligand. As a result of this H-bond net, each perchlorate anion acts as a bridging unit between two complexed dimers (N···O distances <3.33 Å were taken into account). Finally, the crystallization water molecule is roughly equally close to the oxygen atoms O(8) and O(5) provided by two different perchlorate counterions and to the amino nitrogen N(2), the distances being 2.88(1), 2.81(1) and 2.96(1) Å, respectively.

$[Cu_2(L_{-H})_2](ClO_4)_2$ (2, 2′). The asymmetric unit of **2** contains half of the dimeric complex, which is, as a whole, centrosymmetric and a perchlorate ion, while in the asymmetric unit of **2′** there are two halves of the dimeric complex each of which is a centrosymmetric dimer and two perchlorate anions. In **2** as well as in **2′** each copper atom is coordinated by the three nitrogen atoms provided by the same amine ligand and by two oxygen atoms from the phenol moieties one of them provided by the symmetry-related ligand (Figures 2 and 3). These latter donor atoms bridge the two metal ions in the complex, keeping them 3.096(1) Å apart in **2**, while in **2′** the Cu(1)−Cu(1)′ and Cu(2)−Cu(2)′ distances are 3.088(7) and 3.139(7) Å, respectively. The angles Cu(1)−O(1)−Cu(1)′ and Cu(2)−O(2)−Cu(2)′ in **2′** are 98.3(2) and 99.0(2)°, respectively, while in **2** the same angle is 98.4(1)°. In all cases bond distances compare well with those usually found in analogous Cu(II) complexes (Table 3). The coordination sphere around the metal ion in **2** can be described as a trigonal bipyramid (the trigonal index is 0.61) slightly distorted toward the square pyramid (N(3)−Cu(1)−N(2) 135.2(2)°). Considering the sp case, the oxygen O(1) occupies the apex at a distance of 2.145(3) Å, which, as expected, is significantly longer than the Cu−O(1)′ one (1.943(3) Å). In the tbp coordination environment the tertiary nitrogen atom N(1) and the oxygen O(1)′, each one provided by a different ligand, occupy the axial positions, with the metal cation displaced 0.114(1) Å toward the axial oxygen with respect to the equatorial donors. Lowering the temperature causes a slight but significant rearrangement of the coordination sphere about the metal ions in opposite directions (vide infra). As a result two half-independent metal complexes **2′a** and **2′b** were found in the solid-state collected at 80 K (Figure 3). The distortion toward the square pyramid for the dimer **2′a** is slightly marked as provided by the value of the trigonal index τ for the coordination sphere around the Cu(1) metal ion (0.56, N(2)−Cu(1)−N(3) 138.0(3)°).

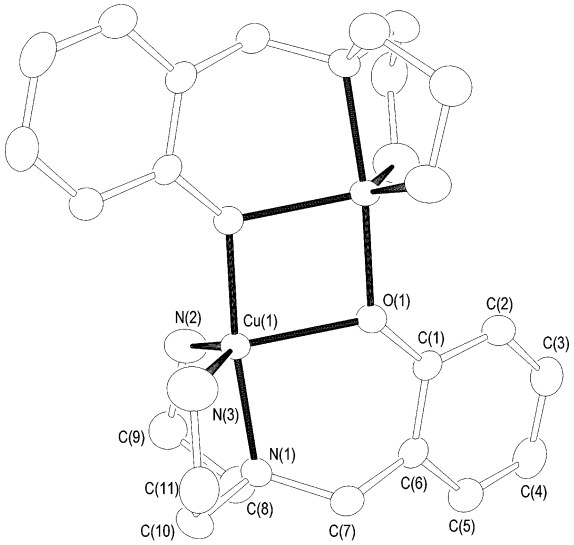

Figure 2. ORTEP-3 view of the centrosymmetric complex cation $[Cu_2(L_{-H})_2]^{2+}$ collected at 298 K. For sake of clarity only the independent atoms were labeled. Thermal ellipsoids are at 30% probability.

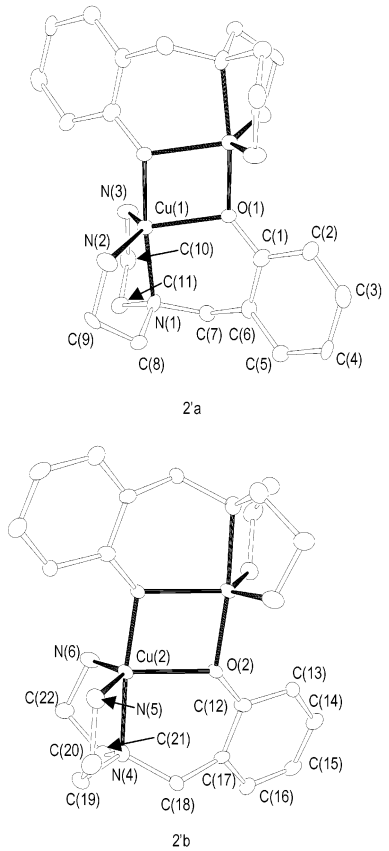

Figure 3. ORTEP-3 view of the two different centrosymmetric complex cations $[Cu_2(L_{-H})_2]^{2+}$ collected at 80 K. [Symmetry operation: **2′a** = $-x + 1, -y, -z$; **2′b** = $-x, -y - 1, -z - 1$.] Thermal ellipsoids are at 30% probability.

Table 3. Selected Bond Lengths (Å) and Angles (°) for 2 and 2′ [a]

2		2′a		2′b	
Cu(1)−Cu(1)*	3.096(1)	Cu(1)−Cu(1)′	3.088(7)	Cu(2)−Cu(2)″	3.139(7)
Cu(1)−O(1)	2.145(2)	Cu(1)−O(1)	2.111(6)	Cu(2)−O(2)	2.160(6)
Cu(1)−O(1)*	1.943(2)	Cu(1)−O(1)′	1.972(6)	Cu(2)−O(2)″	1.966(5)
Cu(1)−N(1)	2.017(3)	Cu(1)−N(1)	2.060(6)	Cu(2)−N(4)	2.047(6)
Cu(1)−N(2)	2.022(3)	Cu(1)−N(2)	2.064(7)	Cu(1)−N(5)	2.039(6)
Cu(1)−N(3)	2.076(3)	Cu(1)−N(3)	2.060(6)	Cu(1)−N(6)	1.991(7)
Cu(1)−O(1)−Cu(1)*	98.4(1)	Cu(1)−O(1)−Cu(1)′	98.3(2)	Cu(2)−O(2)−Cu(2)″	99.0(2)
O(1)*−Cu(1)−O(1)	81.6(1)	O(1)′−Cu(1)−O(1)	81.7(2)	O(2)″−Cu(2)−O(2)	81.0(2)
N(1)−Cu(1)−O(1)	92.1(1)	N(1)−Cu(1)−O(1)	92.7(2)	N(4)−Cu(2)−O(2)	92.9(2)
N(2)−Cu(1)−O(1)	114.9(1)	N(2)−Cu(1)−O(1)	115.1(2)	N(5)−Cu(2)−O(2)	109.2(2)
N(3)−Cu(1)−O(1)	109.0(1)	N(3)−Cu(1)−O(1)	106.1(2)	N(6)−Cu(2)−O(2)	117.0(2)
O(1)*−Cu(1)−N(1)	172.0(1)	O(1)′−Cu(1)−N(1)	171.8(2)	O(2)″−Cu(2)−N(4)	172.0(2)
O(1)*−Cu(1)−N(2)	92.7(1)	O(1)′−Cu(1)−N(2)	92.1(2)	O(2)″−Cu(2)−N(5)	101.1(2)
O(1)*−Cu(1)−N(3)	102.4(1)	O(1)′−Cu(1)−N(3)	102.1(2)	O(2)″−Cu(2)−N(6)	93.5(2)
N(1)−Cu(1)−N(2)	85.4(1)	N(1)−Cu(1)−N(2)	84.8(2)	N(4)−Cu(2)−N(5)	85.8(2)
N(2)−Cu(1)−N(3)	135.2(2)	N(2)−Cu(1)−N(3)	138.0(2)	N(5)−Cu(2)−N(6)	133.2(2)
N(1)−Cu(1)−N(3)	84.4(1)	N(1)−Cu(1)−N(3)	85.2(2)	N(4)−Cu(2)−N(6)	84.5(2)

[a] Symmetry operations: asterisk, $-x+1, -y+1, -z+1$; prime, $-x+1, -y, -z$; double prime, $-x, -y-1, -z-1$.

Also in this case the distance Cu(1)−O(1) is significantly longer than the Cu(1)−O(1′) distance (2.111(6) Å vs 1.972(6) Å). On the contrary the coordination environment around Cu(2) is more distorted toward the tbp: $\tau = 0.65$ for the Cu(2) metal ion coordination environment, N(5)−Cu(2)−N(6) = 133.2(3)°, and the distances Cu(2)−O(2) and Cu(2)−O(2′) are respectively 2.160(6) and 1.966(5) Å. Finally, in both the independent complexes Cu(1) and Cu(2) cations are 0.108(3) and 0.096(3) Å displaced toward O(1′) and O(2′), respectively.

In both **2** and **2′** a lot of intermolecular contacts involve the oxygen atoms of the perchlorate ions and the hydrogen atoms of the primary nitrogen atoms of the ligand.

$[Zn_2(L_{-H})_2(ClO_4)_2]$ (3). The asymmetric unit contains the dinuclear complex and two independent perchlorate anions. Each zinc ion is coordinated by three nitrogen atoms from the ligand and two oxygen atoms from the phenol moieties, these latter bridging the two metal ions which are 3.140(2) Å apart (see Figure 4). The distances Zn···O and Zn···N are in agreement with those found for analogous compounds retrieved in the CSD (Table 2). The coordination geometry of each metal cation, which resembles that of the Cu(II) ion in the homologous complex, results in a distorted trigonal bipyramid ($\tau = 0.55$), with N(1) [N(4)] and O(2) [O(1)] provided by two different ligands at the apexes of the pyramid surrounding the Zn(1) [Zn(2)] ion. Both the tbp are quite distorted toward a square pyramidal geometry as provided by the angles between the axial donors which are slightly bent, 165.1(4)° for O(2)−Zn(1)−N(1) and 163.4(3)° for O(1)−Zn(2)−N(4), and the opening of the O(1)−Zn(1)−N(3) and O(2)−Zn(2)−N(5) angles (131.9(4) and 130.7(4)°, respectively). Both the metal cations are displaced toward the axial oxygen atoms with respect to the equatorial donors (0.165(1) and 0.172(1) Å for Zn(1) and Zn(2), respectively). The atoms O(1), O(2), Zn(1), and Zn(2) are well placed in a plane, the maximum deviation being 0.014(8) Å, for O(2). The planes described by the phenol moieties form an angle of 122.0(5)°.

There are lots of intermolecular contacts between the oxygen atoms of the perchlorate anions and the hydrogen atoms provided by the primary amino groups of the ligand (donor−acceptor distances less than 3.25 Å were taken into account). Particularly, a perchlorate oxygen atom [O(4)] bridges two nitrogen atoms of the two different ligands of a complex, while the oxygen O(7) of the other independent counterion bridges two dinuclear complexes.

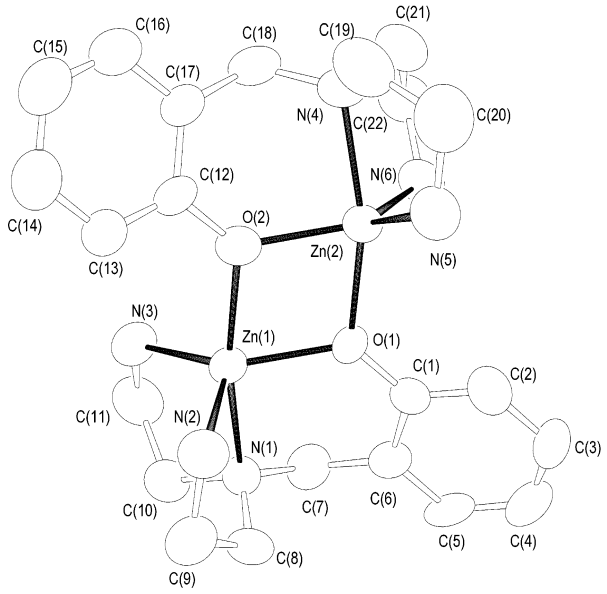

Figure 4. ORTEP-3 view of the complex cation $[Zn_2(L_{-H})_2]^{2+}$. Thermal ellipsoids are at 30% probability.

For comparative purposes, a search in the CSD was performed to retrieve Ni(II), Cu(II), and Zn(II) dimeric five-coordinated complexes (M···M distance ranges from 2.0 to 3.5 Å). Few complexes (ca. 30) of the M_2L_2 type were found, most of them being Cu(II) dimers, some Zn(II), and only one involving two nickel cations. In all cases four donor atoms (N and/or O) are provided by the chelating ligand, one of which, usually the oxygen atom of a phenol moiety, bridges the two metal ions. These latter are kept to a mean distance of 3.17(2) and 3.18(2) Å, for Cu(II) and Zn(II) dimers, respectively.

Conversely solid-state data deposited in the CSD demonstrate that the addition of guest species by the M_2L_2 complex

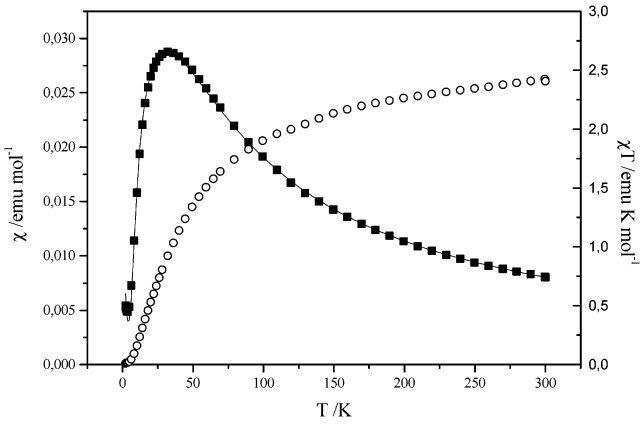

Figure 5. Thermal dependences of the χ (■) and χT (○) for complex **1**. The solid line represents the fitting curve.

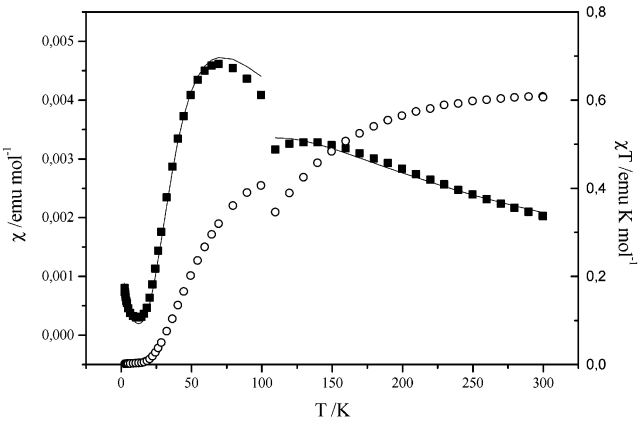

Figure 6. Thermal dependences of the χ (■) and χT (○) for complex **2**. The solid line represents the fitting curve.

is quite common if L possesses only three donor atoms, to complete the coordination sphere of both the metal ions which are usually in a 5-coordinate surrounding.

In this respect, in previous studies we had shown[13c,29] that dinuclear complexes of Cu(II), Ni(II), and Zn(II) ions with the related symmetric ligand **L1** bearing two [bis(2-aminoethyl)amino]methyl arms in the 2 and 6 positions of the phenol grouping are able to assemble external species both in the solid state and in solution, the host molecule being recognized by the two metal cations which act as assemblers.

Also in this study the dimeric dinuclear complexes could be able to assemble external species so to increase the metal coordination number up to 6, with minor rearrangement of the whole complex, as the solid-state structure of **1** suggests.

Interestingly, few solid-state structures of dinuclear metal complexes of transition metal cations with a perchlorate oxygen atom acting as a bridge between two ions (metal−oxygen distances less than the sum of the metal and oxygen van der Waals radii) have been deposited at the CSD, and none of them involves Ni(II) species, while most of them feature mercury, silver, and copper ions.

Although **L** is a quite simple ligand, the way the two M**L** complexes self-assemble in the dimer are quite different in the M_2L_2 species here presented. In fact, taking into account a square pyramidal (sp) environment for each metal ion in all the complexes, it has been noticed that in **1** the two sp are related by a noncrystallographic plane passing through O(1)−C(1)−O(2)−C(12); in **2** and **2′** they are symmetry-related by an inversion center with the oxygen atom at the apex of the sp. The same holds in **3** but with N(2) and N(6) at the apexes of the sp about Zn(1) and Zn(2), respectively. Thus, **L** appears to be a quite versatile ligand in assembling together metal cations.

Magnetic Data. The temperature dependences of the magnetic susceptibilities and χT product of compounds **1** and **2** on the absolute temperature are shown in Figures 5 and 6, respectively. For **1** the maximum value of χ observed around 32 K is indicative of an antiferromagnetic coupling between the nickel(II) ions. For **2** a discontinuity of the χ vs T curve was measured at 99 K. This feature is characteristic of a phase transition induced by the temperature, and it is in agreement with the change in the unit cell parameters observed in the X-ray diffraction experiments performed in function of the temperature. An overall antiferromagnetic interaction is in any case operative between the copper(II) centers. Magnetic data were in any case interpreted using the Hamiltonian isotropic exchange spin $H = JS_1 \cdot S_2$. For **1** the measured temperature dependence of the magnetic susceptibility was fitted using[25]

$$\chi = Ng^2\mu_B{}^2 \frac{2e^{-(J/KT)}}{1 + 3e^{-(-J/KT)}}(1 - \rho) + \frac{2Ng^2\mu_B{}^2}{3KT}\rho \quad (1)$$

where ρ is the percentage of monomeric impurity. Intermolecular interactions were empirically taken into account using the formalism of the molecular field as[25]

$$\chi' = \frac{\chi}{1 + (J_{int}/Ng^2\mu_B{}^2)\chi} \quad (2)$$

where χ is the magnetic susceptibility computed with eq 1 and J_{int} is the interdimer effective exchange interaction. The data were fitted by minimizing the square of differences between observed and computed values divided by the computed values using the MINUIT program package. The results of the fitting are shown in Figure 5 as solid lines. The best fit parameters were $g = 2.32(1)$, $J = 21.84(2)$ cm^{-1}, $J_{int} = 8.42(2)$ cm^{-1}, and $\rho = 1.03(4)\%$. Zero-field splitting effects were not explicitly taken into consideration since it is well-known that these effects can be masked by interdimer interactions and it is more important for ferromagnetic coupling.

For **2** the measured temperature dependence of the magnetic susceptibility was fitted with the procedure previously described with two different sets of parameters for data from 4.2 to 90 K and from 99 to 300 K, using[25]

$$\chi = Ng^2\mu_B{}^2 \frac{2e^{-(J/KT)} + 10e^{-(3J/KT)}}{1 + 3e^{-(-J/KT)} + 5e^{-(3J/KT)}}(1 - \rho) + \frac{Ng^2\mu_B{}^2}{4KT}\rho \quad (3)$$

ρ has the same meaning as in eq 1. Interdimer interactions were applied using eq 2. The results of the fitting are shown

(29) Dapporto, P.; Formica, M.; Fusi, V.; Giorgi, L.; Micheloni, M.; Paoli, P.; Pontellini, R.; Rossi, P. *Inorg Chem.* **2001**, *40*, 6186.

Table 4. Protonation Constants (log *K*) of **L** Determined in 0.15 mol dm^{-3} NaCl Aqueous Solution at 298.1 K

reacn	log *K*
$\mathbf{L}_{-H}^{-} + H^{+} = \mathbf{L}$	11.06(1)[a]
$\mathbf{L} + H^{+} = H\mathbf{L}^{+}$	9.85(1)
$H\mathbf{L}^{+} + H^{+} = H_2\mathbf{L}^{2+}$	8.46(1)
$H_2\mathbf{L}^{2+} + H^{+} = H_3\mathbf{L}^{3+}$	2.38(2)

[a] Values in parentheses are the standard deviations in the last significant figure.

in Figure 6 as solid lines. The low-temperature parameters are $g = 2.16(1)$, $J = 97.68(4)$ cm^{-1}, $J_{int} = 10.08(3)$ cm^{-1}, and $\rho = 3.05(3)\%$. The high-temperature data were fitted with $g = 2.01(1)$, $J = 136.91(4)$ cm^{-1}, $J_{int} = 1.00(1)$ cm^{-1}, and $\rho = 3.03(3)\%$. These data well agree with the change of copper(II) ion coordination geometry observed by solving the molecular structure collected at 80 K. Down to 100 K we have only one copper(II) site, while after the structural phase transition two nonequivalent copper(II) sites are present, i.e., two nonequivalent dimers, and we observed that the average behaviors of these two are both different for the high-temperature one, as described in detail in the structural section. In both cases the parameters used to reproduce the magnetic behavior agree well with cases[30,31] of similar coordination sphere and geometrical parameters.

Compound **1** is EPR silent. Room-temperature EPR spectra of compound **2** are characterized by an intense $\Delta M_s = \pm 2$ transition at $g_{eff} = 4.93$ and a large band at $g_{eff} = 2.04$, which can be assigned to the monomeric impurity (3% by previous calculation). Other less intense features appeared on cooling attributable to transitions within the $S = 1$ states of the dimers. We did not try to assign the spectra since the number of parameters required for the two nonequivalent dinuclear units exceeds the number of observed transitions.

Solution Studies. Basicity. Table 4 summarizes the basicity constants of **L** potentiometrically determined in aqueous 0.15 mol dm^{-3} NaCl solution at 298.1 K. Due to the presence of the phenolic function, the ligand can lose the hydroxyl proton which is thus present in solution as anionic $\mathbf{L}_{-H}^{-}$ species. With examination of the stepwise basicity constants starting from this species, $\mathbf{L}_{-H}^{-}$ can bind up to four protons in the pH range 2−11 investigated, giving rise to the fully protonated species $H_3\mathbf{L}^{3+}$.

The ligand shows a high basicity constant value for the addition of the first proton to the $\mathbf{L}_{-H}^{-}$ species and quite high values for the second and third basicity constants (log $K_2 = 9.85$ and log $K_3 = 8.46$, respectively) while a gap of approximately 6 log units occurs in the fourth protonation step (log $K_4 = 2.38$). This trend of values suggests that the first three protonation steps involve sites located far from each other to minimize the electrostatic repulsion, helped by the open structure of **L**. Moreover, the remarkably high first value can be explained by taking into account that the addition of the proton occurs on an anionic species.

(30) Spiro, C. L.; Lambert, S. L.; Smith, T. J.; Duesler, E. N.; Gagnè, R. R.; Hendrickson, D. N. *Inorg. Chem.* **1981**, *20*, 1229.
(31) Crawford, V. H.; Richardson, H. W.; Wasson, J. R.; Hodgson, D. J.; Hatfield, W. E. *Inorg. Chem.* **1976**, *15*, 2107.

Table 5. Logarithms of the Equilibrium Constants Determined in 0.15 mol dm^{-3} NaCl at 298.1 K for the Complexation Reactions of **L** with Ni(II), Cu(II), and Zn(II) Ions

	log *K*		
reacn	Ni(II)	Cu(II)	Zn(II)
$M^{2+} + \mathbf{L}_{-H}^{-} = M\mathbf{L}_{-H}^{+}$	14.80(1)[a]	19.12(2)	15.07(2)
$M^{2+} + \mathbf{L}_{-H}^{-} + H^{+} = M\mathbf{L}^{2+}$	20.80(3)	25.54(1)	
$M^{2+} + \mathbf{L}_{-H}^{-} + 2H^{+} = MH\mathbf{L}^{3+}$		27.62(7)	
$M^{2+} + \mathbf{L}_{-H}^{-} + H_2O = M\mathbf{L}_{-H}OH + H^{+}$	3.56(3)	8.76(2)	4.39(2)
$M^{2+} + \mathbf{L}_{-H}^{-} + 2H_2O = M\mathbf{L}_{-H}(OH)_2^{-} + 2H^{+}$		−1.78(3)	
$2M^{2+} + 2\mathbf{L}_{-H}^{-} = (M\mathbf{L}_{-H})_2^{2+}$	31.25(5)	40.96(3)	32.23(4)
$2M^{2+} + 2\mathbf{L}_{-H}^{-} + H_2O = M_2(\mathbf{L}_{-H})_2OH^{+} + H^{+}$		31.70(3)	

[a] Values in parentheses are the standard deviations in the last significant figure.

UV−vis absorption electronic spectra of **L** in aqueous solutions performed at different pH values gave further information about the role of the phenolic function in the acid−base behavior of **L**. The spectra show that below pH 7, where the $H_2\mathbf{L}^{2+}$ and $H_3\mathbf{L}^{3+}$ species are present in solution, the phenolic function is in its neutral form (band with λ_{max} at 273 nm and $\epsilon = 2600$ cm^{-1} mol^{-1} dm^3, characteristic for the neutral form of phenol). On the contrary, above pH 8, where the $H\mathbf{L}^{+}$, **L,** and $\mathbf{L}_{-H}^{-}$ are present, the spectra are characteristic for the anionic phenolate form (two bands with λ_{max} at 235 and 292 nm and $\epsilon = 9100$ and 4200 cm^{-1} mol^{-1} dm^3, respectively). In other words, the deprotonation of the hydroxyl function occurs in the pH range which involves the $H_2\mathbf{L}^{2+}$and the $H\mathbf{L}^{+}$ species; thus, the $H\mathbf{L}^{+}$ and **L** species are present in solution in their zwitterionic form, furnishing a separation of the positive and negative charges.

Coordination of Metal Ions. The coordination behavior of **L** toward the bipositive metal cations Ni(II), Cu(II), and Zn(II) was studied in aqueous 0.15 mol dm^{-3} NaCl solution at 298.1 K. The stability constants for the equilibrium reactions were determined potentiometrically, and the data are reported in Table 5. $\mathbf{L}_{-H}^{-}$ forms the mononuclear species $[M\mathbf{L}_{-H}]^{+}$ with all the three metals here investigated. All of the mononuclear $[M\mathbf{L}_{-H}]^{+}$ species self-assemble by forming a dinuclear species with stoichiometry $[M_2(\mathbf{L}_{-H})_2]^{2+}$. The distribution diagrams of the species of the three **L**/M(II) systems as a function of pH are shown in Figure 7. As expected, the mononuclear complex $[Cu\mathbf{L}_{-H}]^{+}$ shows higher stability than the Ni(II) and Zn(II) complexes having the same stoichiometry, which show approximately the same formation constants. The **L**/Cu system gives the presence of complexed species also at low pH. In fact while Ni(II) shows the formation of a monoprotonated $[Ni\mathbf{L}]^{2+}$ (log $K =$ 20.80) and of the $[Ni\mathbf{L}_{-H}]^{+}$ (log $K = 14.80$) species and Zn(II) only the formation of the $[Zn\mathbf{L}_{-H}]^{+}$ species (log $K =$ 15.07) at slightly acidic pH, the **L**/Cu(II) system gives a mono- $[M\mathbf{L}]^{2+}$ and a diprotonated $[MH\mathbf{L}]^{3+}$ species which are present even at low values of pH (Figure 7). All the $[M_2(\mathbf{L}_{-H})_2]^{2+}$ species are forming in solution together with the mononuclear one (see Figure 7), thus suggesting that the formation of $[M_2(\mathbf{L}_{-H})_2]^{2+}$ species is due to the self-assembling of the $[M\mathbf{L}_{-H}]^{+}$ species. This aspect suggests that in the $[M\mathbf{L}_{-H}]^{+}$ species the ligand does not complete the coordination requirement of the ion, which can be saturated

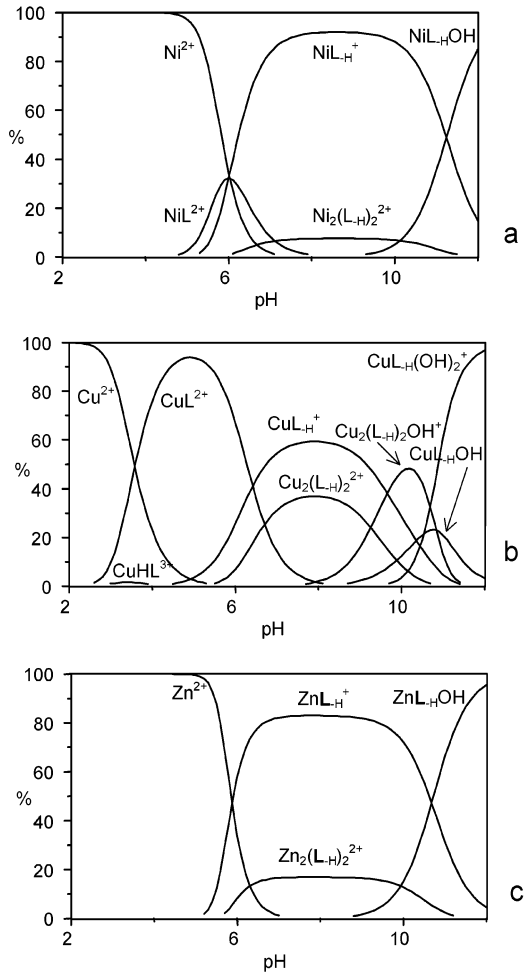

Figure 7. Distribution diagrams of the species for the system **L**/M(II) as a function of pH in aqueous solution ($I = 0.15$ mol dm^{-3} NaCl, at 298.1 K, [**L**] $= 1 \times 10^{-3}$ mol dm^{-3}, [M^{2+}] $= 1 \times 10^{-3}$ mol dm^{-3}: **L**/Ni(II) (a); **L**/Cu(II) (b); **L**/Zn(II) (c).

binding an external species in this case, another mononuclear species. The propensity to form the dinuclear species is a little more marked for the Cu(II) complex but important also for the other two metals. The self-assembling reactions of two $[M\mathbf{L}_{-H}]^+$ mononuclear species give formation values of log $K = 1.65$, 2.72, and 2.09 for $[Ni\mathbf{L}_{-H}]^+$, $[Cu\mathbf{L}_{-H}]^+$, and $[Zn\mathbf{L}_{-H}]^+$, respectively. This particular aspect of two mononuclear species assembled together is due to the presence in **L** of the phenol moiety, which plays a fundamental role in the formation of the dinuclear complexes. In fact, the capacity of the phenolic oxygen, as phenolate, to bridge two metal ions permits each phenolate of each mononuclear species to bridge two metals, one belonging to one mononuclear species and one to the other. In this way the phenolate of one mononuclear species completes the coordination requirement of the metal ion of the other mononuclear species and vice versa. In this way, the two metals should have a coordination arrangement similar to that found in the solid state for all the three crystal structures reported. The mononuclear species must be preorganized for their self-assembling, taking into account that the dinuclear adducts are formed in competition with the addition of water molecules and hydroxide anion to saturate the coordination vacancy of the metal in the mononuclear species.

Given the formation constants of **L** with those of the other ligands depicted in Chart 1, it is possible to suppose that in each mononuclear species $[M\mathbf{L}_{-H}]^+$ the metal is bound by all four donor atoms of **L**.[13,32] We can suppose that in the mononuclear species $[M\mathbf{L}_{-H}]^+$ the metal is tetracoordinated but, due to the conformation of the ligand, it does not achieve a stable tetrahedral conformation giving an open area prone to the coordination of at least another external species. The presence of at least one hydroxylated $[M\mathbf{L}_{-H}OH]$ species confirms this hypothesis.

To understand the role played by the phenolic function in the formation of complexes, UV spectra were recorded in aqueous solutions containing **L** and M(II) at different pH values. For example, in the analysis of the spectra for the system **L**/Cu(II), the spectrum recorded at pH 5.5, where the $[Cu\mathbf{L}]^{2+}$ species is prevalent in solution, shows two bands, one sharp at λ_{max} at 271 ($\epsilon = 2800$ cm^{-1} mol^{-1} dm^3) and one large at 646 nm ($\epsilon = 100$ cm^{-1} mol^{-1} dm^3). The first band is due to the $\pi\angle\pi^*$ transition of the phenol when it is in its neutral form, and the other is due to the copper d−d electron transfer. These data suggest that in the $[Cu\mathbf{L}]^{2+}$ species the phenol is not strongly involved in the coordination. On the contrary, the spectrum recorded at pH 8, where the mono- and dinuclear species are present in solution, shows four bands at λ_{max} 242 (sharp, $\epsilon = 8400$ cm^{-1} mol^{-1} dm^3), 293 (sharp, $\epsilon = 5300$ cm^{-1} mol^{-1} dm^3), 384 (sharp, $\epsilon = 300$ cm^{-1} mol^{-1} dm^3), and 740 nm (large, $\epsilon = 130$ cm^{-1} mol^{-1} dm^3). The two bands at higher energy are due to the $\pi\angle\pi^*$ transitions of the phenolate; the band at 384 nm is ascribed to the phenolate−copper charge transfer when the oxygen atom bridges two Cu(II) ions,[33] while a large band with λ_{max} 740 nm is again due to the d−d electron transfer of the metal. These data indicate the involvement of the oxygen of the aromatic chromophore as phenolate in the stabilization of the complex and, moreover, that it bridges the two metals in the dinuclear species.

Similar features were found for the other two metal complexes which, however, cannot show the diagnostic band of phenol−metal electron transfer.

The ^{1}H and ^{13}C NMR spectra of the $[Zn_2(\mathbf{L}_{-H})_2](ClO_4)_2$ species recorded in methanol solution show a series of signals due to a C_s symmetry of the complex in solution mediated on the NMR time scale (see Experimental Section). On lowering of the temperature up to −70 °C, the spectral features do not change, denoting the presence of only one species in solution. The spectra can be attributed to the dinuclear species, taking into account that the MS (ESI) spectrum performed on the methanol solution gives the predominant presence of the dinuclear complex (see Experimental Section). In other words, the methanol solvent shifts the equilibrium mono/dinuclear species toward the last one, favoring the almost total presence of the dinuclear complex

(32) Smith, R. M.; Martell, A. E. *Critical Stability Constants*; Plenum Press: New York, 1975, p 2; 1982 1st supplement.
(33) Berends, H. P.; Stephen, D. W. *Inorg. Chem.* **1987**, *26*, 749.

in solution. Similar MS-ESI spectra were found for the other two complexes.

These experimental data show that the presence of an unsaturated coordination environment for all three metals in the $[M\mathbf{L}_{-H}]^+$ mononuclear species leads to the self-assembling of two of those species in solution. This is mainly ascribed to the capacity of the phenolic oxygen to bridge two metal ions and to the complementary binding sites in the mononuclear species, which allow the two metal ions to assemble very close to each other. It is of note that the tendency of two mononuclear species to self-assemble is the same for all the three $[M\mathbf{L}_{-H}]^+$ species investigated. This aspect could open the route for the formation of dinuclear complexes formed by two different metal ions. For example, by the mixing of two mononuclear $[M\mathbf{L}_{-H}]^+$ species of two different M′ and M″ metal ions, it could be possible to form a $[(M'M''(\mathbf{L}_{-H})_2]^{2+}$ heterodinuclear species having particular chemical properties. Moreover, the easy obtaining of the solid complexes suggests that the $[M\mathbf{L}_{-H}]^+$ species could be used as building blocks for new polymers and materials by separating at least two of them by a spacer.

Concluding Remarks

The molecular topology of ligand **L** is characterized by the presence of one phenol moiety coupled with a triaminic fragment. The anionic $\mathbf{L}_{-H}{}^-$ species can be obtained in strong alkaline solution; this species behaves as tetraprotic base in aqueous solution. The deprotonation of the hydroxyl function occurs at pH higher than 8 giving rise to a separation of the negative and positive charges for $H\mathbf{L}^+$ and **L** species, which are in their zwitterionic form.

Deprotonated species of **L** form stable mononuclear complexes with Ni(II), Cu(II), and Zn(II) ions with $[M\mathbf{L}_{-H}]^+$ stoichiometry. Two $[M\mathbf{L}_{-H}]^+$ species self-assemble in aqueous solution giving rise to a dinuclear $[M_2(\mathbf{L}_{-H})_2]^{2+}$ species. Due to their lower solubility with respect to the mononuclear species, these complexes can be easily isolated in the solid state as diperchlorate salts. The experiments highlighted that the self-assembling of two $[M\mathbf{L}_{-H}]^+$ species is due to the presence at the same time of an unsaturated coordination environment of the metal ion in the mononuclear species and to the capacity of the phenolic oxygen to bridge metal ions thus completing the coordination requirement of each metal and assembling them very close to each other. The tendency of two mononuclear species to self-assemble is the same for all the three $[M\mathbf{L}_{-H}]^+$ species investigated, suggesting the possibility of obtaining heterodinuclear complexes by assembling two different metal ions and of obtaining new polymers and materials, taking into account the fact that the two metal ions are interacting in the complexes. The three crystal structures of the homodinuclear complexes and the magnetic measurements underlined this aspect. Measurements of magnetic susceptibility show, due to their closeness, an antiferromagnetic coupling between Ni(II)−Ni(II) and Cu(II)−Cu(II) in the dinuclear complexes; while the $[Ni_2(\mathbf{L}_{-H})_2]^{2+}$ species is EPR silent, $[Cu_2(\mathbf{L}_{-H})_2]^{2+}$ gives spectra due to such species.

Acknowledgment. Financial support from the MIUR (Grants COFIN2000 and -2001), EC networks 3MD (Grant No. ERB4061PL97-0197), MOLNANOMAG (Grant No. HPRN-CT-1999-0012), and the Italian CNR, CRIST (Centro Interdipartimentale di Cristallografia Strutturale), of the University of Florence and Centre de Diffractométrie de Rennes, where the X-ray measurements were performed, is gratefully acknowledged.

Supporting Information Available: Listings of tables of crystallographic data, positional parameters, isotropic and anisotropic thermal factors, and bond distances and angles in CIF format. This material is available free of charge via the Internet at http://pubs.acs.org.

IC0204070